DR CHIYU SUN (Orcid ID : 0000-0001-5736-4022)

Article type : Research Letter

Title Page

Design and biological evaluation of phenyl imidazole analogs as hedgehog signaling pathway inhibitors

Chiyu Sun,*[a] Ying Zhang,[b] Han Wang,[a] Zhengxu Yin,[a] Lingqiong Wu,[a] Yanmiao Huang,[a] Wenhu Zhang[a], Youbing Wang [a] and Qibo Hu [a]

[a] School of Pharmacy, Shenyang Medical College, Shenyang 110034, China.
[b] School of Chemical Engineering, Shenyang University of Chemical Technology, Shenyang 110142, China.

Corresponding author: scy_dream@126.com,
Tel.: +86-24-62215689,

Acknowledgments

This work was supported financially by Liaoning Science and Technology Project Management (grant number 20170520026); the Science and Technology Fund Project of Shenyang Medical College (grant numbers 20191027).

Conflict of Interest Statement

The authors report no conflict of interest.

Abstract

The hedgehog (Hh) signaling pathway is involved in diverse aspects of cellular events. Aberrant activation of Hh signaling pathway drives oncogenic transformation for a wide range of cancers, and it is therefore a promising target in cancer therapy. In the principle of association and ring-opening, we designed and synthesized a series of Hh signaling pathway inhibitors with phenyl imidazole scaffold, which were biologically evaluated in Gli-Luc reporter assay. Compound **25** was identified to possess high potency with nanomolar IC_{50}, moreover, it preserved the inhibition against wild-type and drug-resistant Smo-overexpressing cells. A molecular modelling study of compound **25** expounded its binding mode to Smo receptor, providing a basis for the further structural modification of phenyl imidazole analogs.

Keywords hedgehog signaling, inhibitors, phenyl imidazole, Smo receptor, modelling

1. Introduction

The Hedgehog（Hh）signaling pathway is not only associated with the maintenance and repair of many human tissues, but also plays an important role in cell growth, survival and metastasis (Sharpe et al., 2015; Makley et al., 2013; Owens et al., 2017; Galperin et al., 2019). Hh signaling is silent in normal cells, however, its abnormal activation is associated with basal cell carcinoma (BCC), medulloblastoma (MB), pancreatic cancer, acute myeloid leukemia (AML), colon and prostate cancer (DeBerardinis et al., 2014; Berman et al., 2002; Mathew et al., 2014;

Cortes et al., 2019; Vesci et al., 2018; Domenech et al., 2012). Aberrant Hh signaling is mainly driven by either ligand-dependent or Patched (Ptch) mutation mechanism, and induces Ptch to release smoothened (Smo) protein, promoting the translocation of its downstream Gli protein into the nucleus to express Hh target gene (Trinh et al., 2014; Mas et al., 2010; Wahid et al., 2016; Salaritabar et al., 2019). Undoubtedly, there is an increasing level of interests in modulating the Hh signaling pathway for cancer treatment.

Smo is the most studied Hh pathway component as a drug target, and its inhibition leads to down-regulation of those genes associated with cancer growth and progression. Most Hh pathway inhibitors suppress the function of Smo receptor. To date, Vismodegib (**1**), Sonidegib (**2**) and Glasdegib (**3**) have been the Smo antagonists approved by the U.S. Food and Drug Administration (FDA) for the treatment of BCC and AML (Angelaud et al., 2016; Robarge et al., 2009; Lindsley, 2016; Oan et al., 2010; Munchhof et al., 2012; Sheridan, 2019) (Figure 1). Despite the significant accomplishment in the development of Hh pathway inhibitors, the clinical use of **1** and **2** is severely restricted by virtue of their several adverse effects including diarrhea, taste disturbance, hair loss and muscle spasms (Ghirga et al., 2018). Alternatively, acquired resistance to these drugs has become a major barrier for their continued advancement (Pricl et al., 2015). For instance, Smo D473H mutation was discovered from metastatic BCC and MB patient with relapse after treatment with **1** (Yauch et al., 2009; Dijkgraaf et al., 2011). Smo D477G, a comparable murine Smo mutant, in the mouse MB model was drug-resistant as well (Coni et al., 2013). Albeit Smo mutation has no effect on Hh signal transduction, it diminished the affinity of ligands to Smo receptor and disrupted their binding. This finding highlights the continued efforts and interests in research and development of novel chemotype Hh pathway inhibitors.

Figure 1 should be here.

In the past decade, some benzimidazole analogs as potential Hh inhibitors have been discovered by the high-throughput screening campaign, for instance, compound **3**, HhAntag691 and SANT-2 (Bariwal et al., 2019). HhAntag691 has been early reported by Curis and Genentech as a potent Hh inhibitor with low nanomolar affinity for SMO (Romer et al., 2004). SANT-2 is a known Smo antagonist with an IC_{50} of 98 nM in the Shh light II assay (Chen et al., 2002). Later, lead optimization of SANT-2 identified TC132 (**4**) with an IC_{50} value of 80 nM, slightly more potent than SANT-2. Büttner et al reported that exchange of benzimidazole core in compound 4 with other heterocyclic rings, such as indole, benzothiazole and benzoxazole, led to decrease in activity (Büttner et al., 2009). Therefore, benzimidazole is an efficacious moiety for Hh inhibition.

In addition, the benzyloxy group was regarded as a bioactive structure normally found in antineoplastic agent like lapatinib (**5**) (Petrov et al., 2006). In our effort to probe novel Hh pathway inhibitors, we introduced benzyloxy moiety into compound **4** to replace the metabolically labile trimethoxy groups (Figure 2). Encouragingly, this modification led to compound **6** with enhanced anti-Hh activity as measured in Gli-Luc reporter assay (IC_{50} of 0.07 μM as comparison to 0.09 μM for compound **4**). In an attempt to further pursue the chemical structural space, replacement of benzimidazole with phenyl imidazole moiety obtained compound **25** according to ring-opening strategy. The emergence of a rotatable bond between phenyl and imidazole was able to reduce its rigidity, which was expected to improve Smo-binding affinity. The recent determination of Smo-vismodegib crystal structures (PDB code 5L7I) allowed us to examine the interaction patterns between the ligands and Smo receptor (Byrne et al., 2016). The predicted Smo-binding affinity of compound **25** was superior to compound **4**, because their docking score were -11.65 kcal/mol and -8.49 kcal/mol, respectively. In this study, a series of phenyl imidazole derivatives were prepared, and their evaluation on Hh signaling pathway inhibition was reported.
Figure 2 should be here.

2. Results and discussion

The synthetic routes for the target compounds were outlined in Schemes 1-2. Methylparaben was etherified with substituted benzyl bromide in acetone to afford compounds **6a-l**, which was hydrolyzed to the key intermediates **7a-l** in refluxing ethanol for 2 hours. The intermediate 3-(1H-benzo[d]imidazol-2-yl)-4-chloroaniline was synthesized in accordance to the reported procedure (Büttner et al., 2009), before its amidation with **7a-l** gave the target compounds **12-16**. 2-chloro-5-nitrobenzonitrile reacted with sodium methylate and ammonium chloride in alkaline conditions to form amidine hydrochloride **9**. Then, the intermediate **10** was obtained via condensation of **9** and 2-bromoacetophenone. **10** and stannous chloride refluxed in acidic ethanol solution, and its reduction product was intermediate **11**. Finally, **11** reacted with **7a-l** to give the target compound **17-28**.
Scheme 1 should be here.
Scheme 2 should be here.

The target compound involoved the following three regions: A, B and a linker. Region A contained benzimidazole moiety and phenyl imidazole moiety. Region B involved

benzyloxyphenyl group. The amide bond was the linker. The inhibitory activity of compound **12-28** on Hh signaling pathway was evaluated by Gli-Luc reporter kit. Compound **1** was positive control and compound **4** was lead compound. The results expressed as half maximal inhibitory concentration (IC_{50}) values and are presented in Table 1. Initially, region A in the tested compounds was focused. Delightedly, the phenyl imidazole derivatives exhibited more potency as compared with the benzimidazole counterparts (**12** vs **18**, **13** vs **19**, **14** vs **26**, **15** vs **27** and **16** vs **24**), indicating that ring-opening structural modification enhanced their Hh inhibition. Further investigations were performed to study the effect of different substituents on the phenyl ring (region B) on Hh inhibition. The introduction of fluoro atom (**22**) or methyl (**27**) in the para-position was superior to trifluoromethyl surrogate (**18**). Ortho-fluoro (**24**) derivative exhibited improved potency than ortho-chlorine analogue (**19**). Besides, meta-fluoro derivative (**25**, IC_{50} = 0.01 μM) displayed higher activity as compared to other electron-withdrawing groups such as meta-trifluoromethyl (**23**, IC_{50} = 0.02 μM) and meta-chlorine (**28**, IC_{50} = 1.16 μM). Moreover, the anti-Hh activity of fluoro atom in the meta- position (**25**) was stronger as compared to that in ortho- (**24**, IC_{50} = 0.04 μM) or para-position (**22**, IC_{50} = 0.43 μM). Although double chlorine substituents (**20**, **21** and **26**) were effective against Hh signaling, they were inferior in potencies to **25**. Compared with **4**, four of the target compounds (**20**, **23**, **24** and **25**) showed higher potency with IC_{50} values less than 0.06 μM. Compound **25** was identified as the most potent compound in this study. More importantly, the potency of compound **25** was 2-fold higher as compared to **1**, suggesting that it was a promising Hh pathway inhibitor.

Table 1 should be here.

The Hh inhibitory activities of this series of compounds probably attributed to their interaction with Smo, since compound **25** effectively competed with BODIPY-cyclopamine in CHO-K1 cells overexpressing wild-type (WT) Smo, with IC_{50} values of 17 nM (Figure 3). Next, it was hypothesized that **25** might be active against the drug-resistant Smo mutant, therefore, we over-expressed both WT mouse Smo and its mutant D477G with GFP in the NIH3T3-Gli-Luc reporter cell line. Consistent with previous reports, mutation of Smo can confer resistance to **1**. As presented in Figure 4, compound **1** suppressed WT Smo-overexpressing cells with an IC_{50} of 20 nM, however, its inhibition of mutant Smo-overexpressing cells declined sharply. On the contrary, compound **25** inhibited WT and mutant Smo-overexpressing cells with similar potencies (IC_{50} = 14 nM for WT, IC_{50} = 25 nM for mutant). The 2-fold shift in IC_{50} indicated that the D477G mutation did not significantly interfere with the binding of **25** to Smo. Next, the cytotoxicity assay

on Hh-driven cancer cells was performed (Figure 5). DAOY cell lines were a suitable human MB model with constitutive Hh activation, which was reported to be resistant to **1** in vitro. Although **1** was less active against DAOY cells, compound **25** apparently decreased proliferation and survival of DAOY cells. Moreover, the cell viabilities of **25** were 51 % and 32 % at concentrations of 1 μM and 10 μM, respectively.

Figure 3 should be here.

Figure 4 should be here.

Figure 5 should be here.

To further elucidate the binding mode of this series of compounds with Smo receptor, a detailed molecular docking study was performed. The predicted binding affinity of compound **25** was the most among all, with the docking score of − 11.65 kcal/mol (Table S1). As shown in Figure 6A, compound **1** (yellow) bound in the pocket closer to the upper opening of Smo, and the binding orientations of compound **1** and **25** (blue) superimposed well with each other. In the binding mode (Figure 6B and 6C), these two compounds shared similar hydrogen bond with Arg400 to amide bond, and Tyr394 shared to nitrogen atom of pyridine or imidazole. In accordance with pyridine ring on **1**, imidazole ring on **25** allowed π-π interaction with Phe391 and Trp281. These common interactions suggested the importance of imidazole ring and amide bond in region A and linker. Differently, the fluorine on **25** formed a hydrogen bond with Lys395. The phenyl rings in region A and B formed π-π interaction with Trp281 and Phe484. Similar results were observed in the conformations of other compounds (Figure S1). The computational modeling study explained the preferable Hh inhibition of compound **25** at the molecular level.

Figure 6 should be here.

3. Conclusion

In summary, a series of structural modified phenyl imidazole analogs are designed on the basis of pharmacological association and ring-opening strategy. The synthesized compounds were evaluated in Gli-luciferase assay, and compounds **20**, **23**, **24** and **25** exhibited more potent activity than the lead compound TC132. In particular, compound **25** showed the highest Hh inhibitory potency with an IC_{50} value of 0.01 μM, which was 2-fold higher than the launched drug vismodegib. Our preliminary investigation indicated that meta-fluoro benzyloxy group was well

tolerated for enhancement of activity in the target compounds. Additionally, both wild-type and mutant Smo were effectively suppressed by **25**, and it displayed moderate antiproliferation against DAOY cells in vitro. Computational simulations offered the molecular basis for rationalizing Hh inhibition of the phenyl imidazole derivatives. Further studies on the structural optimization of these derivatives are currently underway in our laboratory.

References

Angelaud, R., Reynolds, M., Venkatramani, C., Savage, S., Trafelet, H., Landmesser, T., Demel, P., Levis, M., Ruha, O., Rueckert, B., & Jaeggi, H. (2016). Manufacturing development and genotoxic impurity control strategy of the hedgehog pathway inhibitor vismodegib. *Org Process Res Dev*, *20*, 1509-1519. doi: 10.1021/acs.oprd.6b00208

Bariwal, J., Kumar V., Dong, Y.X., & Mahato, R. I. (2019). Design of hedgehog pathway inhibitors for cancer treatment. *Med Res Rev*, *39*, 1137-1204. doi: 10.1002/med.21555

Berman, D.M., Karhadkar, S.S., Hallahan, A.R., Pritchard, J.I., Eberhart, C.G., Watkins, D.N., Chen, J.K., Cooper, M.K., Taipale, J., Olson, J.M., & Beachy, P.A. (2002). Medulloblastoma growth inhibition by hedgehog pathway blockade. *Science*, *297*, 1559-1561. doi: 10.1126/science.1073733

Büttner, A., Seifert, K., Cottin, T., Sarli, V., Tzagkaroulaki, L., Scholz, S., & Giannis, A. (2009). Synthesis and biological evaluation of SANT-2 and analogues as inhibitors of the hedgehog signaling pathway. *Bioorg Med Chem*, *17*, 4943-4954. doi: 10.1016/j.bmc.2009.06.008

Byrne, E. F., Sircar, R., Miller, P. S., Hedger, G., Luchetti, G., Nachtergaele, S., Tully, M. D., Mydock-McGrane, L., Covey, D. F., Rambo, R. P., Sansom, M. S., Newstead, S., Rohatgi, R., & Siebold, C. (2016). Structural basis of smoothened regulation by its extracellular domains. *Nature*, *535*, 517-522. doi: 10.1038/nature18934

Chen J.K., Taipale J., Young K.E., Maiti T., & Beachy P.A. (2002). Small molecule modulation of smoothened activity. *Proc Natl Acad Sci U S A*, *99*, 14071-14076. doi: 10.1073/pnas.182542899

Coni, S., Infante, P., & Gulino, A. (2013). Control of stem cells and cancer stem cells by hedgehog signaling: pharmacologic clues from pathway dissection. *Biochem Pharmacol*, *85*, 623-628. doi: 10.1016/j.bcp.2012.11.001

Cortes, J.E., Gutzmer, R., Kieran, M.W., & Solomon, J.A. (2019). Hedgehog signaling inhibitors in solid and hematological cancers. *Cancer Treat Rev*, *76*, 41-50. doi: 10.1016/j.ctrv.2019.04.005

DeBerardinis, A.M., Madden, D.J., Banerjee, U., Sail, V., Raccuia, D.S., DeCarlo, D., Lemieux, S.M., Meares, A., & Hadden, M.K. (2014). Structure-activity relationships for vitamin d3-based aromatic a−ring analogues as hedgehog pathway inhibitors. *J Med Chem*, *57*, 3724-3736. doi: 10.1021/jm401812d

Dijkgraaf, G.J.P., Alicke, B., Weinmann, L., Januario, T., West, K., Modrusan, Z., Burdick, D., Goldsmith, R., Robarge, K., Sutherlin, D., Scales, S.J., Gould, S.E., Yauch, R.L., & deSauvage, F.J. (2011). Small molecule inhibition of GDC-0449 refractory smoothened mutants and downstream mechanisms of drug resistance. *Cancer Res*, *71*, 435-444. doi: 10.1158/0008-5472.CAN-10-2876

Domenech, M., Bjerregaard, R., Bushman, W., & Beebe, D.J. (2012). Hedgehog signaling in myofibroblasts directly promotes prostate tumor cell growth. *Integr Biol*, *4*, 142-152. doi: 10.1039/c1ib00104c

Galperin, I., Dempwolff, L., Diederich, W.E., & Lauth, M. (2019). Inhibiting hedgehog: an update on pharmacological compounds and targeting strategies. *J Med Chem*, *62*, 8392-8411. doi: 10.1021/acs.jmedchem.9b00188

Ghirga, F., Mori, M., & Infante, P. (2018). Current trends in hedgehog signaling pathway inhibition by small molecules. *Bio Med Chem Lett*, *28*, 3131- 3140. doi: 10.1016/j.bmcl.2018.08.033

Lindsley, C.W. (2016). Novel drug approvals in 2015 and thus far in 2016. *ACS Chem Neurosci*, *7*, 1175-1176. doi: 10.1021/acschemneuro.6b00254

Makley, L.N., & Gestwicki, J.E. (2013). Expanding the Number of ‘Druggable’ Targets: Non-Enzymes and Protein-Protein Interactions. *Chem Biol Drug Des*, *81*, 22-32. doi: 10.1111/cbdd.12066

Mas, C., & Altaba, A.R. (2010). Small molecule modulation of hh-gli signaling: Current leads, trials and tribulations. *Biochem Pharmacol*, *80*, 712-723. doi: 10.1016/j.bcp.2010.04.016

Mathew, E., Zhang, Y.Q., Holtz, A.M., Kane, K.T., Song, J.Y., Allen, B.L., & diMagliano, M.P. (2014). Dosage-dependent regulation of pancreatic cancer growth and angiogenesis by hedgehog signaling. *Cell Rep*, *9*, 484-494. doi: 10.1016/j.celrep.2014.09.010

Munchhof, M.J., Li, Q.F., Shavnya, A., Borzillo, G.V., Boyden, T.L., Jones, C.S., LaGreca, S.D., Martinez-Alsina, L., Patel, N., Pelletier, K., Reiter, L.A., Robbins, M.D., & Tkalcevic, G.T. (2012). Discovery of PF-04449913, a potent and orally bioavailable inhibitor of smoothened. *ACS Med Chem Lett*, *3*, 106-111. doi: 10.1021/ml2002423

Owens, A.E., dePaola, I., Hansen, W.A., Liu, Y.W., Khare, S.D., & Fasan, R. (2017). Design and evolution of a macrocyclic peptide inhibitor of the sonic hedgehog/patched interaction. *J Am Chem Soc*, *139*, 12559-12568. doi: 10.1021/jacs.7b06087

Robarge, K.D., Brunton, S.A., Castanedo, G.M., Cui, Y., Dina, M.S., Goldsmith, R., Gould, S.E., Guichert, O., Gunzner, J.L., Halladay, J., Jia, W., Khojasteh, C., Koehler, M.F.T., Kotkow, K., La, H., LaLonde, R.L., Lau, K., Lee, L., Marshall, D., Marsters, J.C., Murray, L.J., Qian, C.G., Rubin, L.L., Salphati, L., Stanley, M.S., Stibbard, J.H.A., Sutherlin, D.P., Ubhayaker, S., Wang, S.M., Wong, S., & Xie, M.L. (2009). GDC-0449—A potent inhibitor of the hedgehog pathway. *Bioorg Med Chem Lett*, *19*, 5576-5581. doi: 10.1016/j.bmcl.2009.08.049

Romer, J. T., Kimura, H., Magdalena, S., Sasai, K., Fuller, C., Baines, H., Connelly, M., Stewart, C. F., Gould, S., Rubin, L. L., & Curran, T. (2004). Suppression of the Shh pathway using a small molecule inhibitor eliminates medulloblastoma in $Ptc1^{+/-}$ $p53^{-/-}$ mice. *Cancer Cell*, *6*, 229-240. doi: 10.1016/j.ccr.2004.08.019

Salaritabar, A., Berindan-Neagoe, I., Darvish, B., Hadjiakhoondi, F., Manayi, A., Devi, K.P., Barreca, D., Orhan, I.E., Suntar, I., Farooqi, A.A., Gulei, D., Nabavi, S.F., Sureda, A., Daglia, M., Dehpour, A.R., Nabavi, S.M., & Shirooie, S. (2019). Targeting hedgehog signaling pathway: paving the road for cancer therapy. *Pharmacol Res*, *141*, 466-480. doi: 10.1016/j.phrs.2019.01.014

Sharpe, H.J., Wang, W.R., Hannoush, R.N., & deSauvage, F.J. (2015). Regulation of the oncoprotein smoothened by small molecules. *Nat Chem Biol*, *11*, 246 -255. doi: 10.1038/nchembio.1776

Sheridan, M.H. (2019). Glasdegib: first global approval. *Drugs*, *79*, 207-213. doi: 10.1007/s40265-018-1047-7

Trinh, T.N., McLaughlin, E.A., Gordon, C.P., & McCluskey, A. (2014). Hedgehog signalling pathway inhibitors as cancer suppressing agents. *Med Chem Commun*, *5*, 117-133. doi: 10.1039/c3md00334e

Pan, S.F., Wu, X., Jiang, J.Q., Gao, W.Q., Wan, Y.Q., Cheng, D., Han, D., Liu, J., Englund, N.P., Wang, Y., Peukert, S., Miller-Moslin, K., Yuan, J., Guo, R.B., Matsumoto, M., Vattay, A., Jiang, Y., Tsao, J., Sun, F.X., Pferdekamper, A.C., Dodd, S., Tuntland, T., Maniara, W., Kelleher, J.F., Yao, Y.M., Warmuth, M., Williams, J., & Dorsch, M. (2010). Discovery of NVP-LDE225, a potent and selective smoothened antagonist. *ACS Med Chem Lett*, *1*,130-134. doi: 10.1021/ml1000307

Petrov, K.G., Zhang, Y.M., Carter, M., Cockerill, G.S., Dickerson, S., Gauthier, C.A., Guo, Y., Mook, R.A., Rusnak, D.W., Walker, A.L., Wood, E.R., & Lackey, K.E. (2006). Optimization and SAR for dual ErbB-1/ErbB-2 tyrosine kinase inhibition in the 6-furanylquinazoline series. *Bioorg Med Chem Lett*, *16*, 4686-4691. doi: 10.1016/j.bmcl.2006.05.090

Pricl, S., Cortelazzi, B., DalCol, V., Marson, D., Laurini, E., Fermeglia, M., Licitra, L., Pilotti, S., Bossi, P., & Perrone, F. (2015). Smoothened (SMO) receptor mutations dictate resistance to vismodegib in basal cell carcinoma. *Mol Oncol*, *9*, 389-397. doi: 10.1016/j.molonc.2014.09.003

Vesci, L., Milazzo, F.M., Stasi, M.A., Pace, S., Manera, F., Tallarico, C., Cini, E., Petricci, E., Manetti, F., DeSantis, R., & Giannini, G. (2018). Hedgehog pathway inhibitors of the acylthiourea and acylguanidine class show antitumor activity on colon cancer in vitro and in vivo. *Eur J Med Chem*, *157*, 368-379. doi: 10.1016/j.ejmech.2018.07.053

Wahid, M., Jawed, A., Mandal, R.K., Dar, S.A., Khan, S., Akhter, N., & Haque, S. (2016). Vismodegib, itraconazole and sonidegib as hedgehog pathway inhibitors and their relative competencies in the treatment of basal cell carcinomas. *Crit Rev Oncol Hematol*, *98*, 235-241. doi: 10.1016/j.critrevonc.2015.11.006

Yauch, R.L., Dijkgraaf, G.J., Alicke, B., Januario, T., Ahn, C.P., Holcomb, T., Pujara, K., Stinson, J., Callahan, C.A., Tang, T., Bazan, J.F., Kan, Z., Seshagiri, S., Hann, C.L., Gould, S.E., Low, J.A., Rudin, C.M., & deSauvage, F.J. (2009). Smoothened mutation confers resistance to a

hedgehog pathway inhibitor in medulloblastoma. *Science*, *326*, 572-574. doi: 10.1126/science.1179386

Figure legends

Figure 1 Representative structures of Smo inhibitors.

Figure 2 Design strategy of novel phenyl imidazole derivatives.

Scheme 1 (a) substituted benzyl bromide, K_2CO_3, acetone, 80 °C, 5 h; (b)NaOH, aqueous alcohol, 75 °C, reflux, 2 h; (c) (i) $(COCl)_2$, pyridine cat.; (ii) 3-(1H-benzo[d]imidazol-2-yl)-4-chloroaniline, Et_3N, CH_2Cl_2, rt, 12 h.

Scheme 2 (a) (i) CH_3ONa, CH_3OH, -15 °C, 2h; NH_4Cl, 40 °C, 3h, (ii) 2-bromoacetophenone, $NaHCO_3$, THF, reflux, 40 °C, 20h; (c) $SnCl_2 \bullet 2H_2O$, ethanol, HCl, 80 °C, reflux, 8 h; (d) HATU, DIPEA, CH_2Cl_2, **7a-l**, rt, overnight.

Table 1 Hh signaling pathway inhibition of designed compounds

[a] Results expressed as the mean ± standard deviation of three separate IC_{50} determinations. For each determination, concentration-inhibition curves were acquired in triplicate and then averaged to afford a single IC_{50} curve with a 95% confidence interval.

[b] Used as a lead compound.

[c] Used as a positive control.

Figure 3 In vitro inhibition of Smo for compound 25. The values are an average of triplicate separate determinations.

Figure 4 The inhibition of drug-resistant Smo mutant for compound 25. The inhibition of Gli-Luc reporter activity by vismodegib (A) and compound 25 (B) in NIH3T3-Gli-Luc cells overexpressing wild-type Smo or Smo D477G. Error bars represent standard deviation of three parallel groups (n=3).

Figure 5 Cell viability of DAOY cells treated with the indicated doses of vismodegib and compound 25 for 48 h. Data represent the average of three independent experiments.

Figure 6 (A) Overlay of compound 25 (blue) and original ligand vismodegib (yellow) in binding pocket of Smo. (B) Docking conformation of vismodegib (yellow) at the binding site. (C) Docking conformation of compound 25 (blue) at the binding site. Hydrogen bonds are represented by the dashed green lines. The dashed pink lines represent π-π interaction. Surrounding amino acid are shown in grey stick format and labelled.

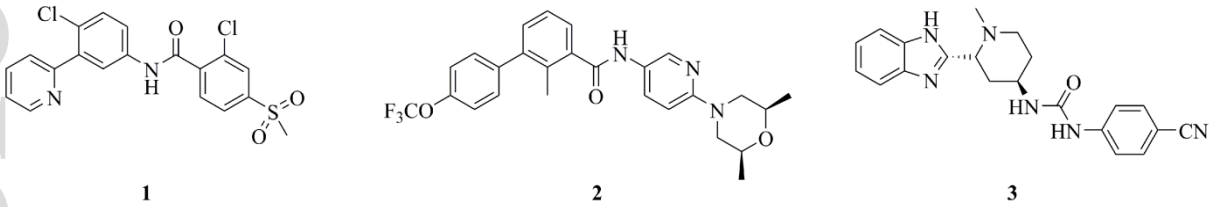

1 **2** **3**

Figure 1

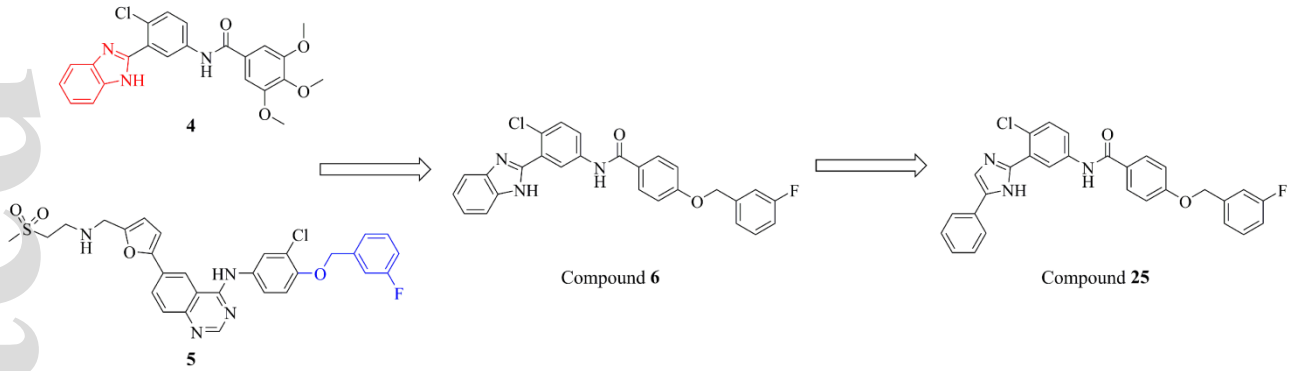

4 **5**

Figure 2

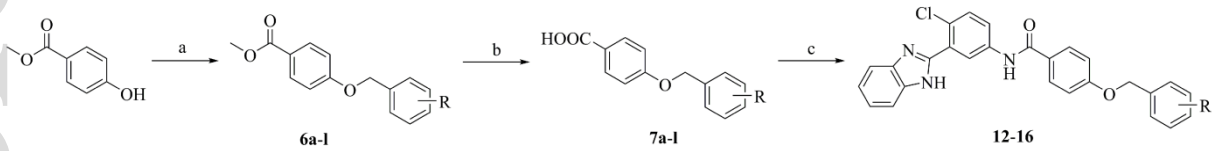

Scheme 1

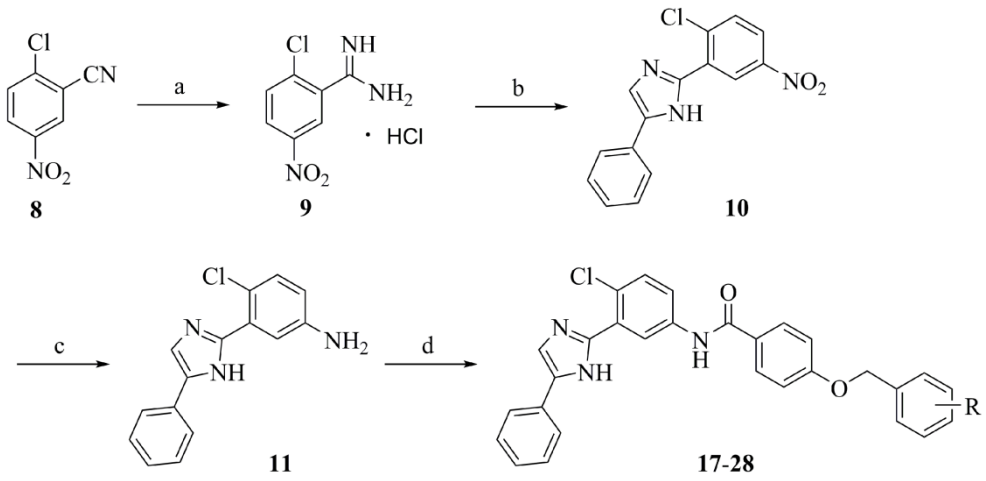

Scheme 2

Talbe 1

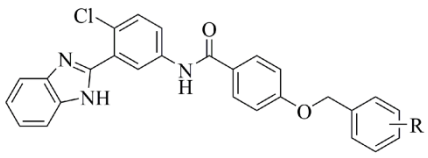

Compound **12-16**

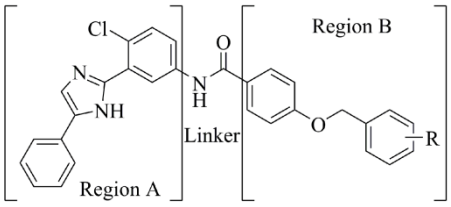

Compound **17-28**

Compd.	R	Gli-luc reporter IC_{50}[a] (μM)	Compd.	R	Gli-luc reporter IC_{50}[a] (μM)
12	4-CF_3	1.86 ± 0.17	22	4-F	0.43 ± 0.05
13	2-Cl	1.30 ± 0.06	23	3-CF_3	0.02 ± 0.01
14	2,4-Cl_2	0.98 ± 0.08	24	2-F	0.04 ± 0.02
15	4-Me	0.75 ± 0.12	25	3-F	**0.01** ± 0.01
16	2-F	0.17 ± 0.05	26	2,4-Cl_2	0.09 ± 0.02
17	-	1.37 ± 0.11	27	4-Me	0.12 ± 0.07
18	4-CF_3	0.62 ± 0.06	28	3-Cl	1.16 ± 0.05
19	2-Cl	0.41 ± 0.03	4[b]	-	0.09 ± 0.01
20	2,3-Cl_2	0.06 ± 0.02	1[c]	-	0.02 ± 0.01
21	3,4-Cl_2	0.29 ± 0.08			

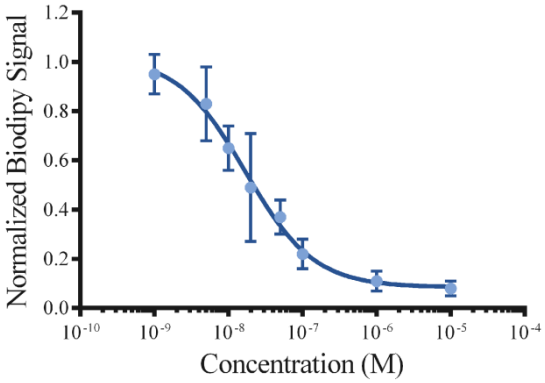

Figure 3

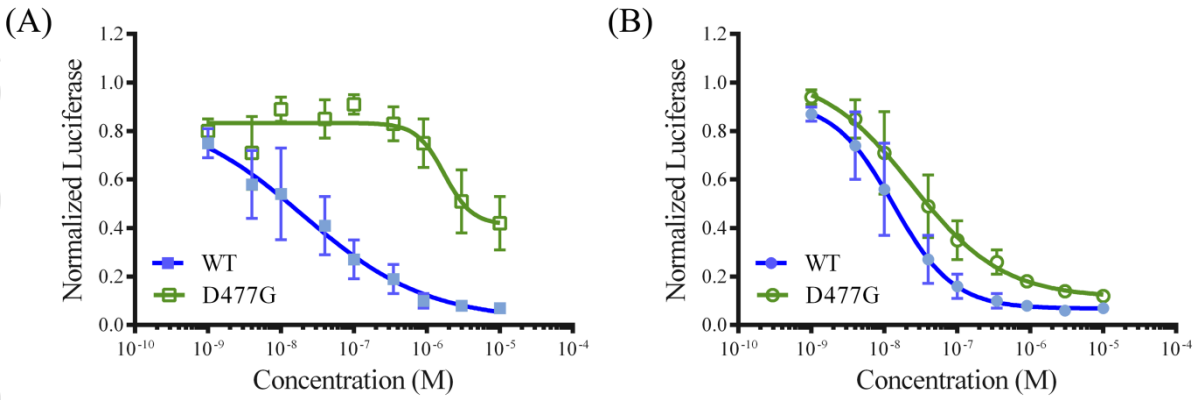

Figure 4

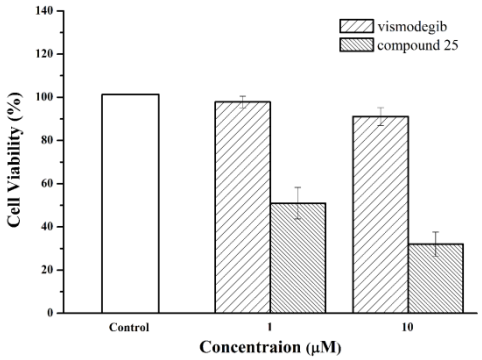

Figure 5

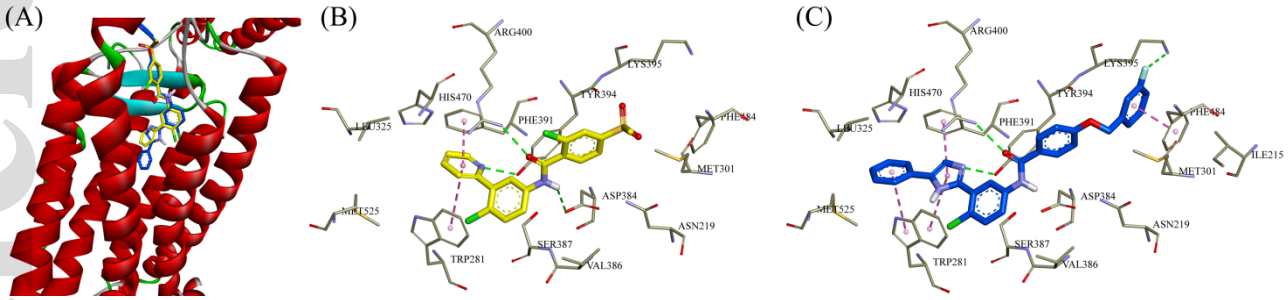

Figure 6

Table 1 Hh signaling pathway inhibition of designed compounds

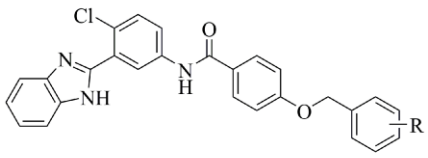

Compound **12-16**

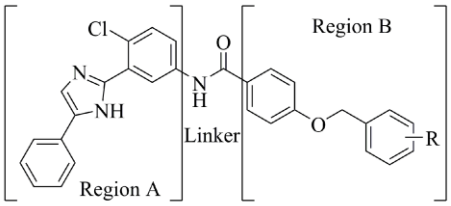

Compound **17-28**

Compd.	R	Gli-luc reporter IC_{50}[a] (μM)	Compd.	R	Gli-luc reporter IC_{50}[a] (μM)
12	4-CF_3	1.86 ± 0.17	22	4-F	0.43 ± 0.05
13	2-Cl	1.30 ± 0.06	23	3-CF_3	0.02 ± 0.01
14	2,4-Cl_2	0.98 ± 0.08	24	2-F	0.04 ± 0.02
15	4-Me	0.75 ± 0.12	25	3-F	**0.01** ± 0.01
16	2-F	0.17 ± 0.05	26	2,4-Cl_2	0.09 ± 0.02
17	-	1.37 ± 0.11	27	4-Me	0.12 ± 0.07
18	4-CF_3	0.62 ± 0.06	28	3-Cl	1.16 ± 0.05
19	2-Cl	0.41 ± 0.03	4[b]	-	0.09 ± 0.01
20	2,3-Cl_2	0.06 ± 0.02	1[c]	-	0.02 ± 0.01
21	3,4-Cl_2	0.29 ± 0.08			

[a] Results expressed as the mean ± standard deviation of three separate IC_{50} determinations. For each determination, concentration-inhibition curves were acquired in triplicate and then averaged to afford a single IC_{50} curve with a 95% confidence interval.

[b] Used as a lead compound.

[c] Used as a positive control.

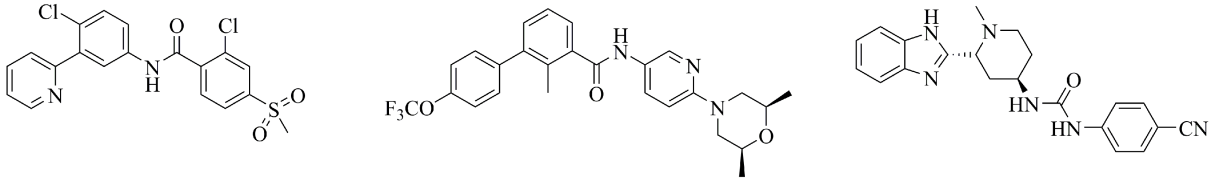

1 **2** **3**

cbdd_13799_f1.tif

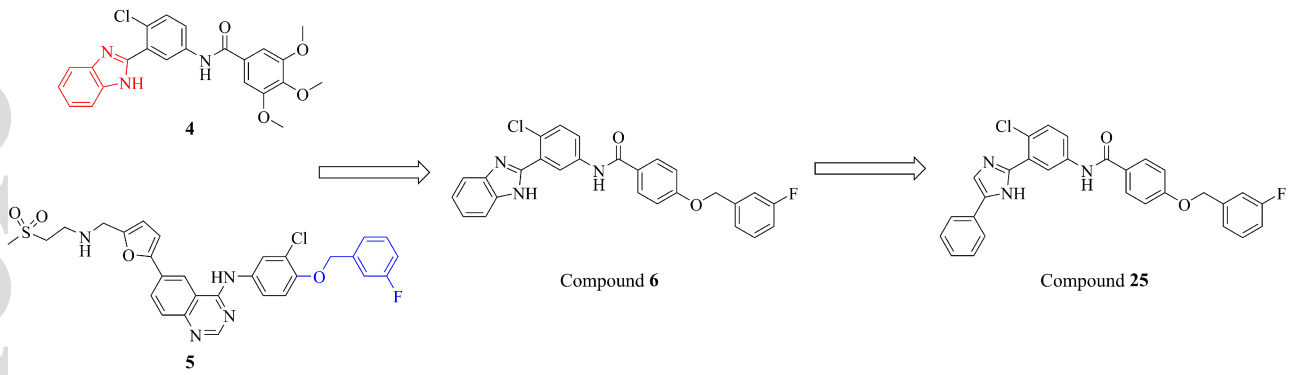

cbdd_13799_f2.tif

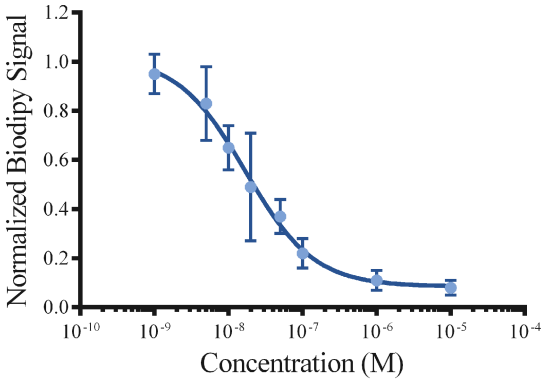

cbdd_13799_f3.tif

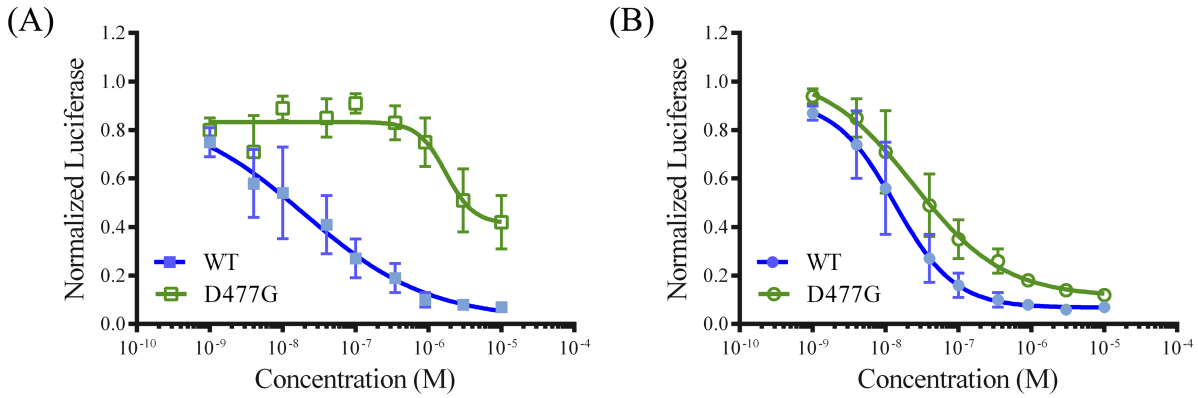

cbdd_13799_f4.tif

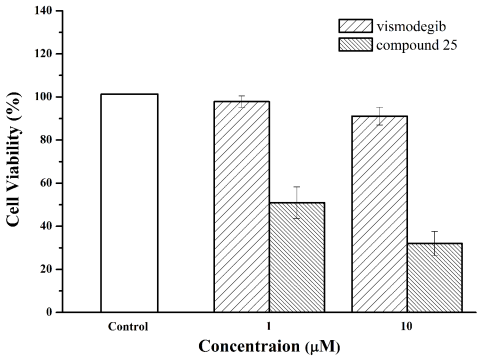

cbdd_13799_f5.tif

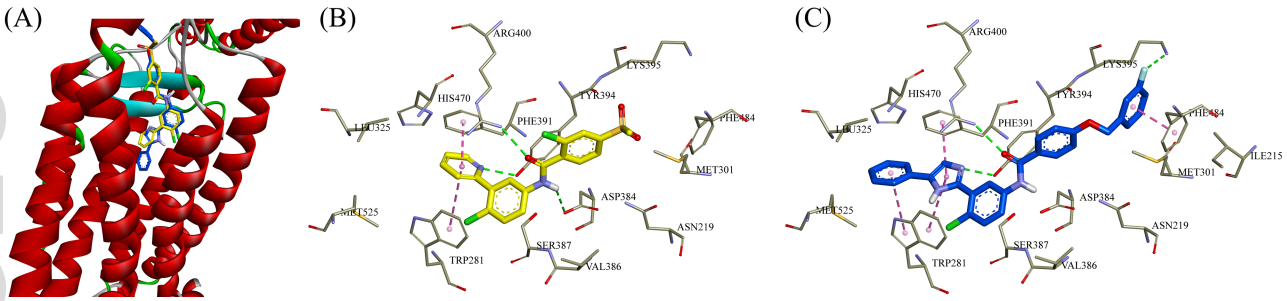

cbdd_13799_f6.tif